JOURNAL OF SOLID STATE CHEMISTRY 105, 580–587 (1993)

Synthesis and Structures of the New Group IV Chalcogenides $NaCuTiS_3$ and $NaCuZrQ_3$ (Q = S, Se, Te)

MICHAEL F. MANSUETTO, PATRICIA M. KEANE, AND JAMES A. IBERS

Department of Chemistry, Northwestern University, Evanston, Illinois 60208-3113

Received October 20, 1992; in revised form December 28, 1992; accepted December 30, 1992

The new compounds $NaCuTiS_3$ and $NaCuZrQ_3$ (Q = S, Se, Te) have been synthesized through reaction of the elements with a Na_2Q_n flux. The compounds $NaCuTiS_3$, $NaCuZrSe_3$, and $NaCuZrTe_3$ crystallize in space group D_{2h}^{16}-*Pnma* of the orthorhombic system with four formula units in cells of dimensions a = 12.738(10), b = 3.554(3), c = 9.529(8) Å for $NaCuTiS_3$; a = 13.392(5), b = 3.833(1), c = 10.250(4) Å for $NaCuZrSe_3$; a = 14.34(4), b = 4.06(1), c = 10.93(3) Å for $NaCuZrTe_3$ (T = 113 K). $NaCuZrS_3$ crystallizes in space group D_{2h}^{17}-*Cmcm* of the orthorhombic system with four formula units in a cell of dimensions a = 3.688(1), b = 12.838(5), c = 9.726(3) Å. The structures of all four compounds have been determined by single-crystal X-ray methods. The structures are composed of $^2_\infty[CuMQ_3^-]$ (M = Ti, Q = S; M = Zr, Q = S, Se, Te) layers separated by Na^+ cations. The Cu atoms are tetrahedrally coordinated and the M atoms are octahedrally coordinated. $NaCuZrS_3$ is isostructural with the recently reported series of compounds $KCuZrQ_3$ (Q = S, Se, Te). $NaCuTiS_3$, $NaCuZrSe_3$, and $NaCuZrTe_3$ represent a new structure type with the $^2_\infty[CuMQ_3^-]$ layer being composed of alternating *pairs* of CuQ_4 tetrahedra and MQ_6 octahedra in the [001] direction. The Na^+ cations are coordinated by seven chalcogen atoms in a monocapped trigonal prismatic arrangement. © 1993 Academic Press, Inc.

Introduction

The use of reactive fluxes for the synthesis of alkali metal/transition metal chalcogenides was first described for the K_2S/S system (*1*). This technique utilizes a low melting alkali metal(A)/chalcogen(Q) flux as a reactant for the synthesis of new materials. These materials often exhibit unusual structures, including one-dimensional (*1–6*) and three-dimensional structures (*6*, *7*) and structures with isolated cations and anions (*8*). The reactive flux technique has been extended to the synthesis of new ternary group IV and V chalcogenides (*1*, *9–13*), quaternary group V sulfides and selenides (*14–16*), and most recently the new quaternary group IV chalcogenides $KCuZrQ_3$ (Q = S, Se, Te) (*17*). Successful substitution of Na for K has afforded another new class of group IV quaternary chalcogenides. Here we describe the synthesis and structures of $NaCuTiS_3$, $NaCuZrS_3$, $NaCuZrSe_3$, and $NaCuZrTe_3$.

Experimental

Syntheses. The compounds $NaCuTiS_3$ and $NaCuZrQ_3$ (Q = S, Se, Te) were prepared by the reactive flux technique. $NaCuTiS_3$ was prepared by combining Na_2S_4 (175 mg, 1.01 mmol; Alfa 90%) with powders of the elements Cu (43 mg, 0.67 mmol; Aldrich 99.9999%) and Ti (32 mg, 0.67 mmol; AESAR 99.9%). $NaCuZrS_3$ was prepared by combining Na_2S (65 mg, 0.83 mmol; Alfa) with powders of the elements Cu (27 mg, 0.42 mmol), Zr (38 mg, 0.42 mmol; AESAR 99%), and S (120 mg, 3.75 mmol; AESAR 99.9999%). The binary starting material Na_2Se_2 was synthesized from reaction of stoichiometric amounts of ele-

0022-4596/93 $5.00

mental Na (Alfa 99.95%) and Se (Aldrich 99.9999%) in liquid ammonia under an argon atmosphere. $NaCuZrSe_3$ was prepared by combining Na_2Se_2 (124 mg, 0.61 mmol) with powders of the elements Cu (26 mg, 0.40 mmol), Zr (37 mg, 0.40 mmol), and Se (64 mg, 0.81 mmol; AESAR 99.9999%). Na_2Te_3 was synthesized by reaction of the elements in stoichiometric quantities at 650°C for 3 days in an evacuated, sealed quartz tube. $NaCuZrTe_3$ was prepared by combining Na_2Te_3 (125 mg; 0.29 mmol) with elemental powders of Cu (19 mg, 0.29 mmol), Zr (13 mg, 0.15 mmol), and Te (93 mg, 0.73 mmol; AESAR 99.5%). The reaction mixtures were loaded into quartz tubes in a dry box under an Ar atmosphere, evacuated to approximately 10^{-4} Torr, and sealed.

For $NaCuTiS_3$, $NaCuZrS_3$, and $NaCuZrSe_3$, the tubes were heated in a furnace from room temperature to 500°C over 12 hr, and held at 500°C for 24 hr. The furnace was then heated to 700°C over 12 hr and held there for 4 days before being cooled to room temperature at 4°C/hr. For $NaCuZrTe_3$ the tube was heated in a furnace at 650°C for 6 days, then ramped to 900°C to heat for 4 days. The furnace was cooled at the rate of 3°C/hr to 450°C and then to room temperature at 90°C/hr.

In all the reactions single crystals formed in the presence of a melt. Very fragile black needles of $NaCuTiS_3$ and black needles of $NaCuZrS_3$ and $NaCuZrSe_3$ were extracted by washing the excess flux away in water. Air-sensitive black needles of $NaCuZrTe_3$ were manually extracted from the melt. The approximate compositions of the compounds were determined by microprobe analyses with an EDAX (Energy Dispersive Analysis by X-rays) equipped Hitachi S570 scanning electron microscope. These analyses confirmed the presence of all four elements in the approximate ratios of 1 : 1 : 1 : 3 for $NaCuTiS_3$, $NaCuZrS_3$, and $NaCuZrSe_3$ and 3 : 1.5 : 1 : 4.5 for $NaCuZrTe_3$.

Structure determinations of $NaCuTiS_3$, $NaCuZrS_3$, $NaCuZrSe_3$, and $NaCuZrTe_3$. Preliminary cell constants and Laue symmetry *mmm* for $NaCuTiS_3$ and $NaCuZrS_3$ were determined from the analysis of Weissenberg photographs collected at room temperature. The systematic absences ($0kl$, $k + l = 2n + 1$; $hk0$, $h = 2n + 1$) are consistent with the orthorhombic space groups D_{2h}^{16} – *Pnma* and C_{2v}^{9} – $Pn2_1a$ for $NaCuTiS_3$ and the systematic absences (hkl, $h + k = 2n + 1$; $h0l$, $l = 2n + 1$) are consistent with the orthorhombic space groups D_{2h}^{17} – *Cmcm*, C_{2v}^{12} – $Cmc2_1$, and C_{2v}^{16} – $C2cm$ for $NaCuZrS_3$. The final cell constants were determined from a least-squares analysis of the setting angles of 30 reflections in the range $17° < 2\theta(MoK\alpha_1) < 26°$ for $NaCuTiS_3$ and 29 reflections in the range $25° < 2\theta(MoK\alpha_1) < 28°$ for $NaCuZrS_3$. For $NaCuZrSe_3$ and $NaCuZrTe_3$ the reflections were in the range $25° < 2\theta(MoK\alpha_1) < 35°$ and $13° < 2\theta(MoK\alpha_1) < 24°$, respectively. The reflections were automatically centered at 113 K on a Picker diffractometer operated from a PC (*18*). The crystals of $NaCuZrTe_3$ are of marginal quality. Six standard reflections monitored every 100 reflections showed no significant change during any of the data collections. Crystal data and other crystallographic details for the four structures are described in Table I.

Intensity data for all compounds were processed and corrected for absorption (*19*) on a Stardent ST2500 computer with programs and methods standard in this laboratory.

The structures of $NaCuTiS_3$, $NaCuZrS_3$, and $NaCuZrSe_3$ were solved with the direct methods program XS in the SHELXTL PLUS program package (*20*). Analysis of the data with the program XPREP (*20*) favored the centrosymmetric space groups *Pnma* for $NaCuTiS_3$ and $NaCuZrSe_3$ and *Cmcm* for $NaCuZrS_3$. The structure of $NaCuZrTe_3$ was solved with the direct methods program SHELX-86 (*21*). $NaCuZrTe_3$ was assumed to be isostructural with $NaCuTiS_3$; therefore the space group *Pnma* was chosen. The program STRUCTURE TIDY (*22*) was used to standardize the positional parameters. The

TABLE I

CRYSTAL DATA AND INTENSITY COLLECTION FOR $NaCuTiS_3$, $NaCuZrS_3$, $NaCuZrSe_3$, AND $NaCuZrTe_3$[a]

Formula	$NaCuTiS_3$	$NaCuZrS_3$	$NaCuZrSe_3$	$NaCuZrTe_3$
Formula mass (amu)	230.6	273.9	414.6	560.6
Space group	D_{2h}^{16}-*Pnma*	D_{2h}^{17}-*Cmcm*	D_{2h}^{16}-*Pnma*	D_{2h}^{16}-*Pnma*
a (Å)	12.738(10)[b]	3.688(1)[b]	13.392(5)[b]	14.34(4)[b]
b (Å)	3.554(3)	12.838(5)	3.833(1)	4.06(1)
c (Å)	9.529(8)	9.726(3)	10.250(4)	10.93(3)
V (Å^3)	431.4	460.5	526.1	636.3
Z	4	4	4	4
ρ_c (g cm^{-3})	3.55	3.95	5.23	5.85
T of data collection (K)[c]	113	113	113	113
Crystal shape	Needle ≈ 0.02 × 0.05 × 0.50 mm bounded by {001}, {100}, {010}, {201}	Needle ≈ 0.02 × 0.04 × 0.26 mm bounded by {001}, {100}, {010}	Needle ≈ 0.02 × 0.03 × 0.21 mm bounded by {001}, {100}, {010}	Needle ≈ 0.02 × 0.08 × 0.16 mm bounded by {100}, {001}, {010}
Crystal volume (mm^3)	5.20×10^{-4}	2.06×10^{-4}	1.38×10^{-4}	2.9×10^{-4}
Linear abs. coeff. (cm^{-1})	78	77	247	183
Transmission factors[d]	0.680–0.844	0.715–0.860	0.476–0.574	0.240–0.664
Detector aperature (mm)	Horizontal, 6.5; vertical, 6.5; 32 cm from crystal	Horizontal, 6.5; vertical, 6.5; 32 cm from crystal	Horizontal, 6.5; vertical, 6.5; 32 cm from crystal	Horizontal, 6.2; vertical, 6.0; 32 cm from crystal
Scan type	ω	θ–2θ	θ–2θ	ω
Scan speed (° min^{-1})	2.0 in ω	2.0 in 2θ	2.0 in 2θ	3.5 in ω
Scan range (°)	−2.10 to +1.40 in ω	−0.60 to +0.70 in 2θ	−0.50 to +0.60 in 2θ	−3.0 to +3.2 in ω
λ^{-1} sin θ, limits (Å^{-1})	0.025 − 0.705 2° ≤ 2θ(Mo$K\alpha_1$) ≤ 60°	0.025–0.747 2° ≤ 2θ(Mo$K\alpha_1$) ≤ 64°	0.025–0.726 2° ≤ 2θ(Mo$K\alpha_1$) ≤ 62°	0.025–0.705 2° ≤ 2θ(Mo$K\alpha_1$) ≤ 60°
Background counts[e]	10 sec each end of scan	10 sec each end of scan	10 sec each end of scan	15 sec each end of scan
Data collected	$\pm h$, $\pm k$, $\pm l$	$\pm h$, $\pm k$, $\pm l$	$\pm h$, $\pm k$, $\pm l$	$\pm h$, $\pm k$, $+l$
No. of data collected	4770	3171	6452	3678
No. of unique data, including $0 \geq F_o^2 \geq -3\sigma(F_o^2)$	721	482	957	999
No. of unique data, with $F_o^2 > 2\sigma(F_o^2)$	534	437	790	560
No. of variables	37	23	37	37
R_{ave}	0.089	0.030	0.053	0.130
$R_w(F^2)$	0.080	0.066	0.076	0.164
R (on F for $F_o^2 > 2\sigma(F_o^2)$)	0.033	0.022	0.026	0.063
Error in observation of unit weight (e^2)	1.06	1.29	1.18	1.52

[a] For all four compounds the radiation was graphite monochromated Mo$K\alpha$ ($\lambda(K\alpha_1)$ = 0.7093 Å, the takeoff angle (°) was 2.5, and the weighting scheme was $w^{-1} = \sigma^2(F_o^2) + (0.04 \times F_o^2)^2$.

[b] Obtained from a refinement so that $\alpha = \beta = \gamma = 90°$.

[c] The low temperature system is based on a design by Huffman (*30*).

[d] The analytical method as employed in the Northwestern absorption program, AGNOST, was used for the absorption correction (*19*).

[e] The diffractometer was operated with the use of the Indiana University PCPS system (*18*).

structures were refined with the use of the program SHELXL92 (*23*) by full-matrix least-squares techniques, the function $\sum w(F_o^2 - F_c^2)^2$ being minimized. Anisotropic thermal motion was included.

For $NaCuTiS_3$ the final refinement led to a value of $R(F_o^2)$ of 0.080. The conventional R index (on F for $F_o^2 > 2\sigma(F_o^2)$) is 0.033. The final difference electron density map shows no features with a height greater than 1% that of a Cu atom. For $NaCuZrS_3$ the final refinement led to a value of $R(F_o^2)$ of

TABLE II

POSITIONAL PARAMETERS AND EQUIVALENT ISOTROPIC THERMAL PARAMETERS FOR $NaCuTiS_3$, $NaCuZrS_3$, $NaCuZrSe_3$, AND $NaCuZrTe_3$

Atom	x	y	z	U_{eq}[a] (Å^2)
		$NaCuTiS_3$		
Na	0.2344(2)	¼	0.0424(3)	0.0147(13)
Cu	0.48691(6)	¼	0.59511(8)	0.0075(4)
Ti	0.01255(8)	¼	0.32621(11)	0.0060(5)
S(1)	0.09493(11)	¼	0.5654(2)	0.0058(7)
S(2)	0.39985(11)	¼	0.3703(2)	0.0061(7)
S(3)	0.36357(11)	¼	0.7637(2)	0.0061(6)
		$NaCuZrS_3$		
Na	0	0.7482(2)	¼	0.0169(10)
Cu	0	0.46692(5)	¼	0.0065(3)
Zr	0	0	0	0.0049(2)
S(1)	0	0.36743(6)	0.05630(9)	0.0055(3)
S(2)	0	0.07682(9)	¼	0.0055(5)
		$NaCuZrSe_3$		
Na	0.2284(2)	¼	0.0421(3)	0.0129(13)
Cu	0.49146(7)	¼	0.59172(8)	0.0079(4)
Zr	0.01178(5)	¼	0.32275(6)	0.0056(3)
Se(1)	0.10368(5)	¼	0.56547(6)	0.0055(3)
Se(2)	0.39470(5)	¼	0.37964(7)	0.0062(3)
Se(3)	0.35962(5)	¼	0.75427(7)	0.0060(3)
		$NaCuZrTe_3$		
Na	0.2269(13)	¼	0.0491(16)	0.029(10)
Cu	0.4919(4)	¼	0.5927(4)	0.016(3)
Zr	0.0110(3)	¼	0.3188(3)	0.013(2)
Te(1)	0.1038(2)	¼	0.5630(2)	0.0118(11)
Te(2)	0.3924(2)	¼	0.3835(2)	0.0133(11)
Te(3)	0.3563(2)	¼	0.7532(2)	0.0124(10)

[a] $U_{eq} = \frac{1}{3}\sum_i\sum_j U_{ij} a_i^* a_j^* \mathbf{a}_i \cdot \mathbf{a}_j$.

0.066. The conventional R index is 0.022. The final difference electron density map shows no features with a height greater than 0.5% that of a Zr atom. For $NaCuZrSe_3$ the final refinement resulted in a value of $R(F_o^2)$ of 0.076. The conventional R index is 0.026. The final difference electron density map shows no peaks greater than 0.8% that of a Zr atom. For $NaCuZrTe_3$ the final refinement led to a value of $R(F_o^2)$ of 0.164. The conventional R index is 0.063. The final difference electron density map shows no features with a height greater than 2.3% that of a Zr atom.

Final values of atomic parameters and equivalent isotropic thermal parameters are summarized in Table II. Final anisotropic thermal parameters and structure amplitudes are available as Supplementary Material.[1]

Results and Discussion

While $NaCuZrS_3$ is isostructural with the recently reported (*17*) $KCuZrQ_3$ series of

[1] See NAPS document No. 05004 for 16 pages of supplementary material. Order from ASIS/NAPS. Microfiche Publications, P.O. Box 3513, Grand Central Station, New York, NY 10163. Remit in advance $4.00 for microfiche copy or $7.75 for photocopy. All orders must be prepaid. Institutions and organizations may order by purchase order. However, there is a billing and handling charge of $15 for this service. Foreign orders add $4.50 for postage and handling, $1.75 for postage of any microfiche orders.

compounds (Q = S, Se, Te)[2], $NaCuTiS_3$, $NaCuZrSe_3$, and $NaCuZrTe_3$ have a different but related structure and are isostructural. In this latter structure $^2_\infty[CuMQ_3^-]$ layers (M = Ti, Q = S; M = Zr, Q = Se or Te) are separated by Na^+ cations. A view down the b axis for $NaCuTiS_3$ given in Fig. 1, shows the stacking of the layers as well as the labeling scheme. Figure 2 shows a $^2_\infty[CuTiS_3^-]$ layer viewed down the a axis.

The $^2_\infty[CuTiS_3^-]$ layer (slab A) is composed of alternating pairs of Ti-centered octahedra and Cu-centered tetrahedra. The Na layer (slab B) consists of Na-centered monocapped trigonal prisms. Within the A slab, the pairs of octahedra are interconnected by edge sharing through an equatorial S(1) atom and an axial S(1) atom in the [001] direction, and edge sharing through equatorial S(1) and S(3) atoms in the [010] direction. The pairs of tetrahedra within a layer are interconnected by edge sharing in the [001] direction through two S(2) atoms, and corner sharing in the [010] direction through one S(2) atom. The octahedra and tetrahedra are connected by edge sharing through

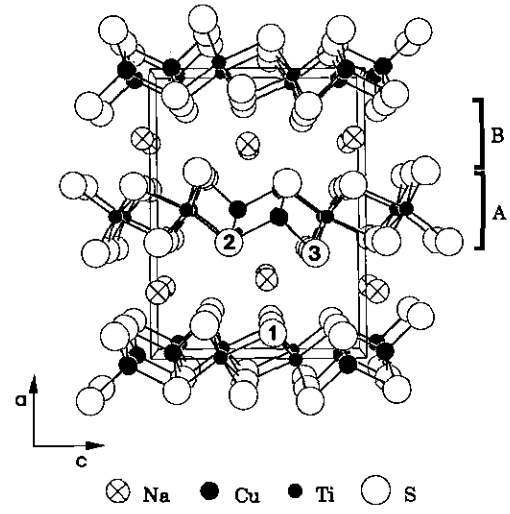

FIG. 1. View down [010] of the structure of $NaCuTiS_3$ with layers and atoms labeled. Here and in Fig. 2 the atoms are shown as circles of arbitrary size.

[2] Also isostructural with this set of compounds is $CsCuZrSe_3$. Cs_2Se_3 was synthesized from reaction of elemental Cs (Aldrich 99.5%) and Se in liquid ammonia under an argon atmosphere. $CsCuZrSe_3$ was prepared by combining Cs_2Se_3 (184 mg, 0.37 mmol) with Cu (16 mg, 0.24 mmol), Zr (22 mg, 0.24 mmol), and Se (29 mg, 0.37 mmol). The heating regime was the same as described above. Black plates of $CsCuZrSe_3$ were extracted by washing the excess flux away in water. From diffractometer data collected at 113 K the compound is found to crystallize in space group *Cmcm* in a cell of dimensions a = 3.898(1), b = 15.831(2), c = 10.197(1) Å. The large increase in the length of the b axis compared with that of $KCuZrSe_3$ (a = 3.874(2), b = 14.506(7), c = 10.159(5) Å (113 K)) reflects the positioning of Cs^+, rather than K^+ ions, in that direction.

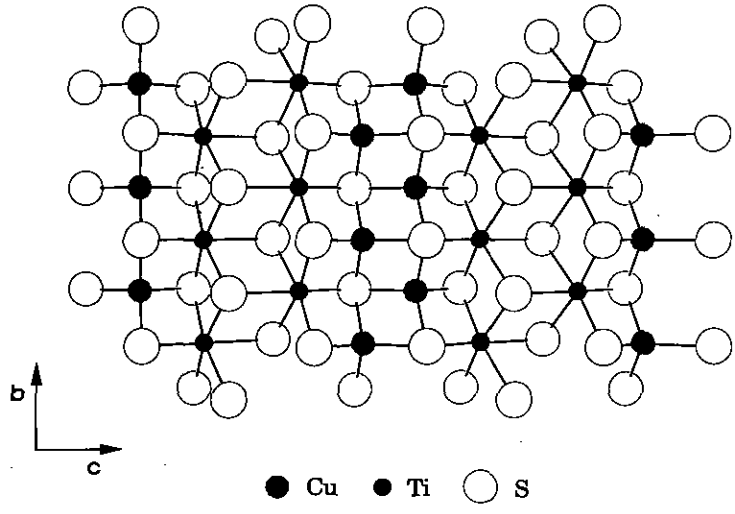

FIG. 2. An isolated $^2_\infty[CuTiS_3^-]$ layer viewed down the [100] direction.

TABLE III

SELECTED DISTANCES (Å) AND ANGLES (°) FOR $NaCuTiS_3$, $NaCuZrSe_3$, AND $NaCuZrTe_3$

	$NaCuTiS_3$	$NaCuZrSe_3$	$NaCuZrTe_3$
Na ··· 2*Q*(1)	2.817(5)	2.965(3)	3.168(15)
Na ··· 2*Q*(2)	2.961(5)	3.027(3)	3.213(14)
Na ··· 2*Q*(3)	3.026(5)	3.129(3)	3.244(15)
Na ··· 1*Q*(3)	3.125(6)	3.434(4)	3.743(19)
Na ··· 1*Q*(2)	3.869(6)	4.115(4)	4.358(19)
Cu–1*Q*(3)	2.247(4)	2.428(2)	2.619(7)
Cu–2*Q*(2)	2.312(3)	2.466(2)	2.635(6)
Cu–1*Q*(2)	2.412(4)	2.531(2)	2.695(7)
Cu–Cu	2.560(4)	2.695(2)	2.878(8)
Cu–*M*	2.830(4)	3.047(2)	3.199(7)
M–1*Q*(2)	2.360(4)	2.600(2)	2.791(7)
M–2*Q*(3)	2.450(4)	2.671(2)	2.873(6)
M–2*Q*(1)	2.470(4)	2.716(2)	2.916(6)
M–1*Q*(1)	2.509(4)	2.776(2)	2.982(8)
Q(1) ··· 2*Q*(1)	3.250(6)	3.631(3)	3.858(8)
Q(1) ··· 2*Q*(2)	3.406(6)	3.747(3)	4.050(9)
Q(1) ··· 2*Q*(3)	3.421(6)	3.754(3)	3.988(9)
Q(1) ··· 1*Q*(3)	3.367(6)	3.755(3)	4.079(10)
Q(2) ··· 2*Q*(2)	3.554(6)	3.833(3)	4.060(11)
Q(2) ··· 2*Q*(3)	3.724(6)	4.047(3)	4.399(9)
Q(2) ··· 1*Q*(3)	3.777(6)	3.869(3)	4.074(11)
Q(3) ··· 2*Q*(3)	3.554(6)	3.833(3)	4.060(11)
Q(3)–Cu–*Q*(2)	109.53(9)	111.58(4)	113.7(2)
Q(2)–Cu–*Q*(2)	100.44(10)	101.98(5)	100.8(3)
Q(3)–Cu–*Q*(2)	108.26(10)	102.54(5)	100.1(3)
Q(2)–Cu–*Q*(2)	114.42(8)	114.76(4)	114.7(1)
Q(2)–*M*–*Q*(3)	101.47(10)	100.32(4)	101.9(2)
Q(3)–*M*–*Q*(3)	92.99(10)	91.72(4)	89.9(2)
Q(2)–*M*–*Q*(1)	89.69(10)	89.62(4)	90.4(2)
Q(3)–*M*–*Q*(1)	168.72(7)	169.87(3)	167.56(1)
Q(3)–*M*–*Q*(1)	86.38(9)	88.37(4)	89.6(2)
Q(1)–*M*–*Q*(1)	92.04(10)	89.76(4)	88.2(2)
Q(2)–*M*–*Q*(1)	167.24(7)	169.24(4)	168.9(2)
Q(3)–*M*–*Q*(1)	87.23(10)	87.11(4)	85.9(2)
Q(1)–*M*–*Q*(1)	81.49(10)	82.78(4)	81.7(2)

an S(2) and S(3) atom in the [001] direction. The CuQ_4 tetrahedra within the layer share edges with two tetrahedra and two octahedra, while the TiQ_6 octahedra share edges with two tetrahedra and four octahedra. Within slab B, the Na-centered monocapped trigonal prisms share triangular faces in the [010] direction. These monocapped trigonal prisms are connected to slab A through edge sharing with both the tetrahedra and octahedra.

Selected interatomic distances and angles for $NaCuTiS_3$, $NaCuZrSe_3$, and $NaCuZrTe_3$ are given in Table III. Distances and angles for $NaCuZrS_3$ are given in Table IV. The Ti–S and Zr–*Q* distances are comparable to those found in TiS_3 (2.358(4) to 2.855(6) Å) (*24*), ZrS_3 (2.602(3) to 2.724(4) Å) (*24*), $ZrSe_3$ (2.71 to 2.87 Å) (*25*), and $ZrTe_3$ (2.771(3) to 3.467(4) Å) (*24*). The Cu–*Q* distances are comparable to those of some known Cu-containing chalcogenides, for example KCu_4S_3 (2.312(2) to 2.451(1) Å) (*26*) and α- and β-$KCuS_4$ (2.298(4) to

TABLE IV

SELECTED DISTANCES (Å) AND ANGLES (°) FOR $NaCuZrS_3$

Na ··· 2S(2)	2.871(3)
Na ··· 4S(1)	3.048(2)
Na ··· 2S(1)	3.329(2)
Cu–2S(1)	2.276(2)
Cu–2S(2)	2.322(2)
Cu–4Zr	3.081(2)
Zr–4S(1)	2.568(2)
Zr–2S(2)	2.624(2)
S(1) ··· 2S(2)	3.576(3)
S(1) ··· 2S(2)	3.765(3)
S(1) ··· 1S(1)	3.576(3)
S(1) ··· 2S(1)	3.688(3)
S(1) ··· 2S(1)	3.700(3)
S(1) ··· 1S(1)	3.768(3)
S(2) ··· 2S(2)	3.688(3)
S(1)–Cu–S(1)	111.73(6)
S(1)–Cu–S(2)	109.94(3)
S(2)–Cu–S(2)	105.16(6)
S(1)–Zr–S(1)	91.77(4)
S(1)–Zr–S(1)	88.23(4)
S(1)–Zr–S(2)	87.05(4)
S(1)–Zr–S(2)	92.95(4)

2.432(4) Å) (*4*), $TlCu_7Se_4$ (2.377(5) to 2.658(3) Å) (*27*) and $TlCu_5Se_3$ (2.389(2) to 2.629(3) Å) (*28*), and Cu_2MTe_3 (2.594(1) to 2.705(1) Å) (*7*). The short Cu–Cu distance of 2.560(4) Å in $NaCuTiS_3$ indicates some Cu–Cu interaction. The remaining Cu–Cu and Cu–Zr distances in $NaCuZrS_3$, $NaCuZrSe_3$, and $NaCuZrTe_3$, however, do not show any significant metal–metal interactions. The closest $Q \cdots Q$ distances of 3.250(6) Å ($NaCuTiS_3$), 3.576(3) Å ($NaCuZrS_3$), 3.631(3) Å ($NaCuZrSe_3$), and 3.858(8) Å ($NaCuZrTe_3$), indicate no significant Q–Q interactions. The MQ_6 octahedra and CuQ_4 tetrahedra are somewhat distorted from their ideal geometries.

The $KCuZrQ_3$ (Q = S, Se, Te) (*17*) and $NaCuZrS_3$ structures differ from the Na $CuMQ_3$ (M = Ti, Q = S; M = Zr, Q = Se or Te) structures in the A slab. The chalcogen framework in the A slab generates several possible metal coordination sites. The nature of these sites is depicted in Fig. 3. For each chalcogen atom there are two tetrahedral sites and one octahedral site. One tetrahedron points "up" and the other points "down." In the $KCuZrQ_3$ and $NaCuZrS_3$ structure a tetrahedral site is filled and then the next two tetrahedra combine to form an octahedron which is filled, resulting in a zigzag chain of alternating ZrQ_6 octahedra and CuQ_4 tetrahedra. In the $NaCuTiS_3$, $NaCuZrSe_3$, and $NaCuZrTe_3$ structure the tetrahedral and octahedral sites are filled resulting in alternating *pairs* of CuQ_4 tetrahedra and MQ_6 octahedra. The geometry of slab B in the two structure types is similar. In the $KCuZrQ_3$ and $NaCuZrS_3$ structure the alkali metal atoms occupy bicapped trigonal prisms. In the other structure type the pairing of the CuQ_4 tetrahedra and MQ_6 octahedra distorts the Q layers to provide a monocapped trigonal prismatic environment for the Na atoms.

The alternation of MQ_6 octahedra and $M'Q_4$ tetrahedra has also been seen in other layered chalcogenides. For example, in the ternary compounds Ta_2NiQ_5 (Q = S, Se)

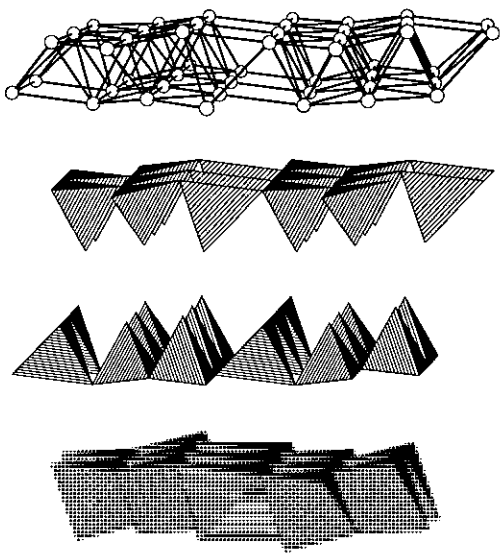

FIG. 3. Depiction of the possible octahedral and tetrahedral vacancies between layers of Q atoms in the A slab in $NaCuMQ_3$ (M = Ti, Q = S; M = Zr, Q = Se or Te).

(*29*) the layers are composed of alternating pairs of Ta octahedra separated by single Ni tetrahedra.

Acknowledgments

This work was supported by the U.S. National Science Foundation through Grant DMR91-14934. Use was made of the SEM facilities of the Northwestern University Materials Research Center supported through U.S. National Science Foundation Grant DMR91-20521.

References

1. S. A. SUNSHINE, D. KANG, AND J. A. IBERS, *J. Am. Chem. Soc.* **109,** 6202 (1987).
2. D. KANG AND J. A. IBERS, *Inorg. Chem.* **27,** 549 (1988).
3. P. M. KEANE AND J. A. IBERS, *Inorg. Chem.* **30,** 1327 (1991).
4. M. G. KANATZIDIS AND Y. PARK, *J. Am. Chem. Soc.* **111,** 3767 (1989).
5. Y. PARK AND M. G. KANATZIDIS, *Angew. Chem. Int. Ed. Engl.* **29,** 914 (1990).
6. M. G. KANATZIDIS, *Chem. Mater.* **2,** 353 (1990).
7. P. M. KEANE AND J. A. IBERS, *J. Solid State Chem.* **93,** 291 (1991).
8. S. SCHREINER, L. E. ALEANDRI, D. KANG, AND J. A. IBERS, *Inorg. Chem.* **28,** 392 (1989).
9. P. M. KEANE, Y.-J. LU, AND J. A. IBERS, *Acc. Chem. Res.* **24,** 223 (1991).
10. E. W. LIIMATTA AND J. A. IBERS, *J. Solid State Chem.* **71,** 384 (1987).
11. E. W. LIIMATTA AND J. A. IBERS, *J. Solid State Chem.* **77,** 141 (1988).
12. E. W. LIIMATTA AND J. A. IBERS, *J. Solid State Chem.* **78,** 7 (1989).
13. S. A. SUNSHINE, D. A. KESZLER, AND J. A. IBERS, *Acc. Chem. Res.* **20,** 395 (1987).
14. Y.-J. LU AND J. A. IBERS, *J. Solid State Chem.* **94,** 381 (1991).
15. Y.-J. LU AND J. A. IBERS, *Inorg. Chem.* **30,** 3317 (1991).
16. Y.-J. LU AND J. A. IBERS, *J. Solid State Chem.* **98,** 312 (1992).
17. M. F. MANSUETTO, P. M. KEANE, AND J. A. IBERS, *J. Solid State Chem.* **101,** 257 (1992).
18. J. C. HUFFMAN, unpublished work.
19. J. DE MEULENAER AND H. TOMPA, *Acta Crystallogr.* **19,** 1014 (1965).
20. G. M. SHELDRICK, "SHELXTL PC, version 4.1. An integrated system for solving, refining, and displaying crystal structures from diffraction data." Siemens Analytical X-Ray Instruments, Inc., Madison, WI.
21. G. M. SHELDRICK, *in* "Crystallographic Computing 3," (G. M. Sheldrick, C. Krüger, and R. Goddard, Eds.), pp. 175–189, Oxford Univ. Press, London (1985).
22. L. M. GELATO AND E. PARTHÉ, *J. Appl. Crystallogr.* **20,** 139 (1987).
23. G. M. SHELDRICK, SHELXL-92 Unix, Beta-Test Version.
24. S. FURUSETH, L. BRATTÅS, AND A. KJEKSHUS, *Acta Chem. Scand. Ser. A* **29,** 623 (1975).
25. W. KRÖNERT AND K. PLIETH, *Z. Anorg. Allg. Chem.* **336,** 207 (1965).
26. D. B. BROWN, J. A. ZUBIETA, P. A. VELLA, J. T. WROBLESKI, T. WATT, W. E. HATFIELD, AND P. DAY, *Inorg. Chem.* **19,** 1945 (1980).
27. L. ERIKSSON, P.-E. WERNER, R. BERGER, AND A. MEERSCHAUT, *J. Solid State Chem.* **90,** 61 (1991).
28. R. BERGER, L. ERIKSSON, AND A. MEERSCHAUT, *J. Solid State Chem.* **87,** 283 (1990).
29. S. A. SUNSHINE AND J. A. IBERS, *Inorg. Chem.* **24,** 3611 (1985).
30. J. C. HUFFMAN, Ph.D. Thesis, Indiana University (1974).